Sparticle mass measurements at ATLAS; calculating three-body endpoints

Candidate Number: 8165T
Supervisor: Chris Lester

Abstract

The kinematic endpoint method for calculating supersymmetric particle masses is extended in this work to find endpoint expressions for the gluino decay which concludes with a three body decay, $\tilde{g} \to \tilde{q}q \to \tilde{\chi}_2^0 qq \to \tilde{\chi}_1^0 qqll$. This decay creates 11 observable endpoints, which will be obtained at ATLAS from the edges of the invariant mass distributions of the visible decay particles. The endpoint positions depend only on the sparticle masses and together they provide enough constraints to reconstruct the sparticle masses. A montecarlo event generator confirmed the expressions in all but two cases. The fundamental assumption underlying the derivations is that $m_{\tilde{g}} > m_{\tilde{q}} > m_{\tilde{\chi}_2} > m_{\tilde{\chi}_1}$ but within this hierarchy the method is applied and tested for all regions of mass space. Therefore the derived endpoints can be used for all models in which this decay chain is produced.

Introduction

Supersymmetry

After decades of planning, the Large Hadron Collider (LHC) at CERN will start collecting data next year. By probing energies not yet achieved in another collider, it is hoped that the ATLAS detector at the LHC will provide the much needed evidence to support the most developed and accepted extension of the Standard Model (SM), known as supersymmetry. The ATLAS detector is one of two general purpose detectors at the LHC, with the primary aims of discovering the Higgs boson and exploring the physics beyond the SM.

As the SM can explain almost all the experimental high energy physics data, it was only relatively recently that work on neutrino oscillations showed the theory to be incomplete. One of the main inadequacies of the SM is the so called hierarchy problem. Corrections to the Higgs mass result from Yukawa couplings between the fermions and Higgs field. These one loop contributions introduce a quadratic sensitivity of the Higgs-mass-squared to the cut-off, Λ_{UV}, which is introduced to regulate the loop integral, (figure 1). If Λ_{UV} is placed at the Planck scale, the Higgs mass becomes 10^{18}Gev rather than the order of 780GeV, which is the upper limit set by unitarity in the SM. Tremendous fine-tuning is then required in the SM to keep the masses low and this is an unsatisfactory solution.

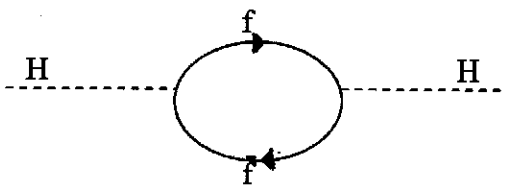

Figure 1. Fermion loop correction to the higgs mass, with coupling strength λ_f

$$\Delta m_H^2 = \frac{|\lambda_f|^2}{16\pi^2}[-2\Lambda_{UV}^2 + 6m_f^2 \ln(\Lambda_{UV}/m_f) + ...] \qquad [a]$$

By introducing a symmetry between fermions and bosons, supersymmetry stabilises the Higgs mass. It states that for every fermion (boson) degree of freedom, there exists a boson (fermion) degree of freedom, with the same non-mass quantum numbers. This introduces 'superpartners' with a spin differing by ½ a unit to all our known SM particles. These partners, must also contribute to the Higgs mass, now with scalar loop diagrams (figure 2) for which the quadratic dependence on Λ_{UV} has the opposite sign to the fermion corrections.

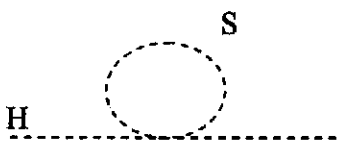

Figure 2. Scalar loop corrections to higgs mass with coupling strength λ_s.

$$\Delta m_H^2 = \frac{\lambda_s}{16\pi^2}[\Lambda_{UV}^2 - 2m_s^2 \ln(\Lambda_{UV}/m_s) + ...] \quad [b]$$

Comparing [a] and [b], it is clear that if $\lambda_s = |\lambda_f|^2$ and there are two scalar loops for every fermion loop, the leading order corrections cancel. Therefore, if two scalar partners, or sparticles, with appropriate coupling constants exist for every fermion, only a logarithmic divergence remains. Conventionally sparticles are presented in literature with a tilde and are named by adding an s to the corresponding SM particle name.

According to the supersymmetric model, each of the fundamental SM particles are either in a chiral or gauge supermultiplet together with their superparnter, which has the same electric charge, weak isospin and colour degrees of freedom. Left and right handed fermions each have a separate scalar partner, which shares the gauge interactions of its fermion, although it does not possess a particular helicity state itself. The squarks and sleptons have spin 0 and reside in chiral supermultiplets with the fermions. The third generations, the stop and bottom squarks and the stau leptons can also mix to form the mass eigenstates.

The Higgs boson also belongs to a chiral supermultiplet, and in fact supersymmetry requires two multiplets, one to give mass to the up-type quarks and one for the down-type quarks. (Table 1)

The SM spin 1 vector bosons are in gauge supermultiplets with their spin ½ superpartners, referred to as gauginos. There are eight gluinos, corresponding to the gluons that mediate QCD interactions. Winos and binos are the massless partners of the bosons, $W^{\pm}, W^0, B^0$. (Table 2) After electroweak symmetry breaking, zino and photino states are formed corresponding to the SM Z^0 boson and photon.

Names		spin 0	spin 1/2
squarks, quarks (×3 families)	Q	$(\tilde{u}_L \ \tilde{d}_L)$	$(u_L \ d_L)$
	$\overline{u}$	$\tilde{u}^*_R$	$u^\dagger_R$
	$\overline{d}$	$\tilde{d}^*_R$	$d^\dagger_R$
sleptons, leptons (×3 families)	L	$(\tilde{\nu} \ \tilde{e}_L)$	$(\nu \ e_L)$
	$\overline{e}$	$\tilde{e}^*_R$	$e^\dagger_R$
Higgs, higgsinos	H_u	$(H^+_u \ H^0_u)$	$(\tilde{H}^+_u \ \tilde{H}^0_u)$
	H_d	$(H^0_d \ H^-_d)$	$(\tilde{H}^0_d \ \tilde{H}^-_d)$

Table 1. Chiral Supermultiplets in the Minimal Supersymmetric Model

Names	spin 1/2	spin 1
gluino, gluon	$\tilde{g}$	g
winos, W bosons	$\tilde{W}^+ \ \tilde{W}^0$	$W^+ \ W^0$
bino, B boson	$\tilde{B}^0$	B^0

Table 2. Gauge Supermultiplets in the Minimal Supersymmetric Model

As no sparticles have ever been detected, soft supersymmetry-breaking must occur to make them heavier than their SM partners. 'Soft' refers to the constraint that the breaking mechanism must not ruin the perfect cancellation of the Higgs mass contributions.

After both electroweak and supersymmetry breaking, further mixing can occur between all the gauginos and higgsinos, (not including the gluino). The mass eigenstates are then 4 neutralinos $\tilde{\chi}^0$ and 2 charginos $\tilde{\chi}^\pm$, numbered according to increasing mass, i.e. $\tilde{\chi}^0_4$ is the heaviest neutralino.

Supersymmetry breaking introduces many more parameters, especially as the breaking mechanism is unknown. In order to simplify the full Minimal Supersymmetric Standard Model from having 124 parameters, assumptions are made to reduce the number to about 5. Consequently there are many models to be considered, each with different reduced parameter sets. Minimal supergravity models (mSUGRA) use gravitational interactions as the basis of the breaking mechanism. Various parameters are unified at the GUT scale resulting in the following set; the scalar mass, m_0, the gaugino mass, $m_{1/2}$, the Yukawa couplings, A_0, the ratio of Higgs expectation values, tanβ and the sign of the SUSY Higgs mass parameter μ. In contrast to this is the Non-Universal Higgs Mass (NUHM) model where the degeneracy of the Higgs multiplets is broken.

There are two types of supersymmetric theories; R-parity conserving or R-parity violating. All supersymmetric particles have R = -1 whereas SM particles have R = +1. Therefore, in R-parity conserving theories, (which are used in this work), sparticles must be produced in pairs and must decay to a lighter sparticle via SM particle emission. Mixing between sparticle and particle states is forbidden. (They can also be annihilated by an anti-sparticle but this is unlikely in the LHC.) At the end of every supersymmetric (SUSY) event, there must be a stable, lightest supersymmetric particle (LSP), which is a prime dark matter candidate. It must be electrically neutral and weakly interacting for it to have escaped detection so far. The collider therefore requires a minimum energy of twice the LSP mass. In order to ensure gauge unification at high energy, sparticles must have a mass below one Tev. The LHC will

collide two 7 Tev proton beams, so is predicted to have enough energy to produce a wide range of sparticles.

A SUSY event at the LHC must be detected purely by the SM particles and missing energy of the LSP. Methods to calculate sparticle masses must therefore require knowledge of only the visible decay products. One such method uses the kinematic endpoints of invariant mass distributions, which depend on the sparticle masses. The distributions of all combinations of SM particles in the decay can be generated from the particles' momenta, which will be detected by ATLAS. This study extends previous work by increasing the length of decay chain and deriving expressions for the extra endpoints it produces, thereby increasing the number of constraints on the SUSY masses.

SUSY events

Depending on the particular model of supersymmetry, decay chains are predicted with varying branching ratios to take place at the LHC. The mSUGRA model suggests that the SUSY particles will mostly decay by sequential two-body decays. However, the NUHM model predicts that chains involving both two and three-body decays will be more common.

There are two main assumptions when considering the decays. The sparticles must always decay to lighter sparticles, so there is always a definite mass hierarchy to the sparticles in the chain. It is also assumed for the purposes of this study that the SM particles have negligible mass.

Previous work on a sequential decay chain within the mSUGRA framework in [1], introduces the endpoint analysis used in this study, [1]. The chain considered involved only two-body decays; $\tilde{q}_L \rightarrow \tilde{\chi}_2^0 q \rightarrow \tilde{l}_R^{\pm} l_{near}^{\pm} q \rightarrow \tilde{\chi}_1^0 l_{far}^{\mp} l_{near}^{\pm} q$ (figure 3).

In [3] a gluino was added to the head of this chain, although not all the observable endpoint expressions were derived;
$\tilde{g} \rightarrow q_{near} \tilde{q}_L \rightarrow \tilde{\chi}_2^0 q_{near} q_{far} \rightarrow \tilde{l}_R^{\pm} l_{near}^{\pm} q_{near} q_{far} \rightarrow \tilde{\chi}_1^0 l_{far}^{\mp} l_{near}^{\pm} q_{near} q_{far}$.

Many different chains can result in the same SM particles and it is important that the kinematic structure within the process is known in order to get reliable constraints on the masses. For example, the chain involving a three-body decay
$\tilde{q}_L \rightarrow \tilde{\chi}_2^0 q \rightarrow \tilde{\chi}_1^0 l^{\mp} l^{\pm} q$ has also been studied in [2], (figure 4).

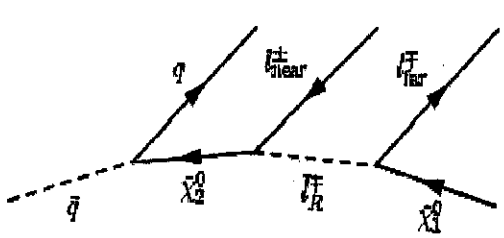

Figure 3. Two-body decay

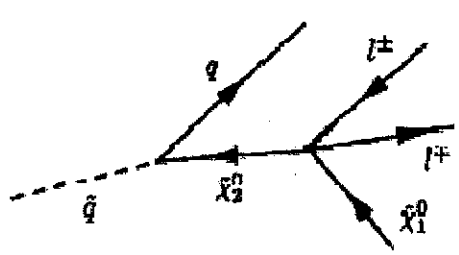

Figure 4. Three-body decay

This produces the same particles as in [1] but the mass distributions have different shapes and consequently endpoints. Therefore, in order for this method to work it must be possible to differentiate between three and two body decays. That is the basis of further work, but, assuming it is possible, it is necessary to obtain expressions for all event scenarios. It was concluded in [2] that there is not enough information from the endpoints to constrain the sparticle masses. There are four endpoints, two of which, the m_{ql} high and low, have a ratio of $\sqrt{2}$. Also in one mass region the m_{qll} endpoint is coincident with the m_{ql} high endpoint. It was found that the m_{qll} threshold would be hard to position accurately and so there is not enough information to evaluate the sparticle masses.

In this work, the chain is extended to include a gluino at the head, as shown in figure 5; $\tilde{g} \rightarrow \tilde{q}q \rightarrow \tilde{\chi}_2^0 qq \rightarrow \tilde{\chi}_1^0 qqll$ [c]. This results in seven further endpoints from which to reconstruct the sparticle masses. All mass regions are considered, meaning that the expressions derived are valid for any combination of sparticles masses, within the constraint that $m_{\tilde{g}} > m_{\tilde{q}} > m_{\tilde{\chi}_2} > m_{\tilde{\chi}_1}$. Therefore these endpoint expressions can be used for all models in which this decay chain occurs. Furthermore, the expressions can be applied, with appropriate re-labelling, to all chains with the same structure, no matter what particles are produced.

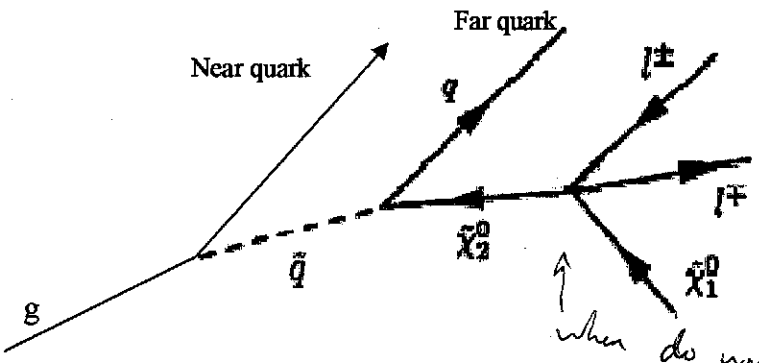

Figure 5: Decay of a gluino, ending with a three-body decay

Method

Decay Simulation

A montecarlo event generator was used to test the theoretical endpoints derived in this paper. (Appendix B) The decay must conserve 4-momentum and the sparticles must decay isotropically to sample all space evenly. For each combination of visible particles, the highest invariant mass found by the simulation is recorded as the simulation endpoint. This can then be compared to the theoretical endpoint. The simulation must not be able to find any event that produces an invariant mass higher than the predicted endpoint.

If the simulation endpoint tends to the theoretical endpoint with increasing number of events, then it can be assumed that with infinite statistics the simulation endpoint would reach the theoretical endpoint.

The theoretical endpoints must cover all regions of parameter space. Therefore the montecarlo program generates completely random sets of sparticle masses, whilst ensuring that $m_{\tilde{g}} > m_{\tilde{q}} > m_{\tilde{\chi}_2} > m_{\tilde{\chi}_1}$ and compares the simulation endpoints to the theoretical predictions for each mass set.

Endpoint Calculation

The endpoints are the maximum values of the invariant mass distributions, and depend only on the sparticle masses. An invariant mass squared of a collection of particles is the sum of their four-momentum squared. For the decay [c] there are eleven invariant mass distributions; m_{qqll}, m_{qq}, m_{ll}, $m_{qql(high)}$, $m_{qql(low)}$, $m_{q_{far}ll}$, $m_{q_{near}ll}$, $m_{q_{near}l(high)}$, $m_{q_{near}l(low)}$, $m_{q_{far}l(high)}$ and $m_{q_{far}l(low)}$. The high and low correspond to the leptons which can not be distinguished in any way, other than the fact that one produces a higher mass than the other. The quarks can be labelled near and far as shown in figure 5. However the ATLAS detector will also be unable to distinguish between the quarks and so in order for the mass distributions to be observable they must be in a form that requires no knowledge of which quark is involved. This replaces the last six distributions above with $m_{qll(high)}$, $m_{qll(low)}$, $m_{ql(huge)}$, $m_{ql(large)}$, $m_{ql(little)}$, and $m_{ql(tiny)}$

When deriving the endpoints, it is necessary to evaluate the magnitude of particles' momenta in a particular rest frame. For a general two-body decay as shown in figure 6, the momenta of the particles in the rest frame of b can be obtained from 4-momentum conservation.

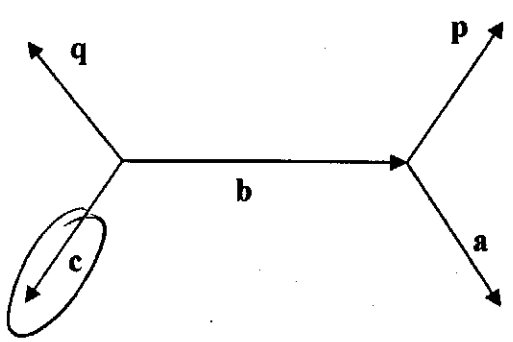

Figure 6

The three momenta, represented throughout with a capital letter, depend on masses $m_{sparticle}$ only, (particle masses are neglected). Consequently the energy $E_{particle}$ can be calculated.

$$P^2 = A^2 = [m_p^2, m_b^2, m_a^2] \qquad [d]$$
$$Q^2 = C^2 = [m_q^2, m_b^2, m_c^2] \qquad [e]$$
$$E_p^2 = m_p^2 + P^2 \qquad [f]$$
$$E_q^2 = m_q^2 + Q^2 \qquad [g]$$

where

$$[x, y, z] = \frac{x^2 + y^2 + z^2 - 2(xy + xz + yz)}{4y}$$

The invariant mass of particles p and q is given by

$$m_{pq}^2 = (p+q)^2$$
$$m_{pq}^2 = m_p^2 + m_q^2 + 2p^\mu q_\mu = m_p^2 + m_q^2 + 2(E_p E_q - |P||Q|\cos\theta) \qquad [h]$$

This is maximised when cosθ is -1, so p and q are back to back in the rest frame of b.

The above are the basic tools needed to be able to derive each endpoint. By combining particles as effective particles and using Lorentz transforms, the successive two-body method can be applied when deriving all the endpoints. See Appendix A for full calculations.

What about the high-low-tion etc?

The endpoint expressions are summarised in Table 3.

The above techniques fail for

The qq and ll endpoints

The m_{ll} edge is the same whether the gluino is at the head of the chain or not, so is the same as that found in [2]. It only depends on the $\tilde{\chi}_2^0$ and $\tilde{\chi}_1^0$ masses as these sparticles and the leptons can be isolated together in the chain.

For the same reason the m_{qq} edge is the same as previously found in [3], despite the end of the chain now having a three-body rather than a two-body decay.

The qqll endpoint → derivation: pg 23 ok ✓

This invariant mass combines all the SM particles and is therefore observable in its current form. It has three possible positions, corresponding to different configurations of the particles relative to one another. Which of these is larger depends on the particular combination of sparticle masses.

The near, far, high and low qll endpoints

When deriving $m_{q_{far}ll}^{\max}$ in [2] the leptons are combined and treated as an effective particle, so to maximise $m_{q_{far}ll}$, the far quark is back to back with m_{ll} in the $\tilde{\chi}_2^0$ rest frame. This is independent of the position of the near quark.

Similarly in order to maximise $m_{q_{near}ll}$, the near quark was found to be back to back with m_{ll} in the squark rest frame. As the far quark is an intermediate particle between the leptons and near quark, the optimum configuration also depends on the far quark's orientation. It was found that the far quark must be back to back with m_{ll} in the $\tilde{\chi}_2^0$ rest frame. Consequently, $m^{\max}_{q_{near}ll}$ and $m^{\max}_{q_{far}ll}$ can occur from the same decay.

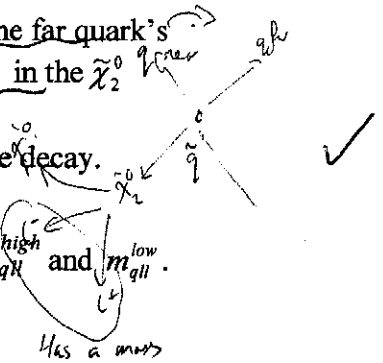

These endpoints must now be converted to observables in the form of m_{qll}^{high} and m_{qll}^{low}.

On an event by event basis

$$m_{qll}^{high} = \max\{m_{q_nll}, m_{q_fll}\}$$
$$m_{qll}^{low} = \min\{m_{q_nll}, m_{q_fll}\}$$

It is not necessary to know which quark produced the edge, just that in each event one of the quarks has a higher invariant mass with the leptons than the other. The high endpoint is the maximum of the high invariant masses and the low endpoint is the maximum of all the low invariant masses.

It is clear to see that

$$m^{\max}_{qll(high)} = \max\{m^{\max}_{q_nll}, m^{\max}_{q_fll}\} = m^{\max}_{q_>ll}$$

as it is not possible for a higher invariant mass to ever be produced. The subscript > has been introduced to denote the quark that produces the higher endpoint. Similarly < is used for the quark which has the lower endpoint.

As $m^{\max}_{q_<ll}$ can originate from an event in which it is the smaller m_{qll}, it is the low endpoint. It is not possible to get a higher endpoint than this, as it would have to be a $m_{q_>ll}$, which can never simultaneously be higher than $m^{\max}_{q_<ll}$ and be in the low position.

$$m^{\max}_{qll(low)} = \min\{m^{\max}_{q_nll}, m^{\max}_{q_fll}\} = m^{\max}_{q_<ll}$$

The ql endpoints

The configuration that maximises $m_{ql(high)}$ for either quark, has the relevant lepton and quark back to back in the squark rest frame (near quark), or the $\tilde{\chi}_2^0$ rest frame (far quark), whilst the other lepton is at rest. The configuration that maximises $m_{ql(low)}$ is similar, except both the leptons are back to back with the quark and have equal

momentum. In the case of the near quark, the direction of the far quark also affects the invariant mass and is found to be back to back with the leptons in the $\tilde{\chi}_2^0$ rest frame too. Therefore, $m^{max}_{q_{far}l(high)}$ is produced from the decay that maximises $m_{q_{near}l(high)}$. The same is true for the low endpoints.

This greatly simplifies matters when thinking about how these endpoints will be observed in ATLAS. The four observable distributions are defined as huge, large, little and tiny. On an event by event basis the four ql masses decrease from $m_{ql(HUGE)}$ to $m_{ql(TINY)}$. The maximum possible values that each of these can take are the four endpoints.

A simple re-ordering of the four unobservable m_{ql} endpoints can be used to find the huge, large and tiny m_{ql} endpoints. However $m^{max}_{ql(LITTLE)}$ is never quite as big as the third highest unobservable m^{max}_{ql}. This is because it is not kinematically possible for the $m_{ql(LITTLE)}$ to approach the corresponding m^{max}_{ql}, whilst simultaneously having the third highest invariant mass. (See appendix for a more detailed discussion). Due to this added complexity, as yet no satisfactory expression has been found for $m^{max}_{ql(LITTLE)}$. The maximum $m_{ql(LITTLE)}$ will occur when the smaller $m_{ql(high)}$ is equal to the larger $m_{ql(low)}$. The leptons in these masses could either be the same lepton or could be different leptons depending on the orientations of all four particles. Therefore deriving this configuration is not a simple task unless assumptions are made. m_{ql} was calculated for the configuration in which the leptons are parallel to one another and back to back with both the quarks as for the low configuration, but now the leptons have unequal momenta. However this was often found to underestimate the endpoint. When this was the case the configuration was investigated by studying the particles' four momenta produced by the simulation. However this showed no obvious pattern so further work is needed to ascertain the optimum configuration.

The high and low qql endpoints

The configuration for these endpoints was assumed to be the same as for the ql endpoints, but with the two quarks combining as an effective particle. This was found to be valid for the high endpoint, leading to four endpoint expressions depending on the value of m_{qq}.

Four similar expressions were found for the low endpoint. However, the simulation showed that other configurations are able to produce larger invariant masses, particularly when $\tilde{\chi}_1^0$ is relatively light compared to the other SUSY masses. The configuration has to be one in which m_{qql} is equal for both leptons as this is when the

lower invariant mass is greatest. This suggests a symmetrical configuration for maximisation, for example when $\tilde{\chi}_1^0$ is produced at rest and the leptons are back to back with each other and perpendicular to $m_{qq}^{\max}$ in the $\tilde{\chi}_2^0$ frame. The quarks are back to back in the squark rest frame and so the line of the two quarks is parallel to the leptons in the $\tilde{\chi}_2^0$ rest frame. The resulting endpoint is only greater than the four other endpoints when the leptons have sufficient momentum in this configuration to compensate for no longer being back to back with the qq particle. Although the addition of the fifth endpoint expression greatly improves the correlation between the theoretical and simulation endpoints, (see analysis), there are still configurations with higher endpoints showing that the real optimum configuration may be close to that described above, but with the $\tilde{\chi}_1^0$ not at rest and therefore the leptons not exactly back to back.

Can this config be drawn?

Table 3; Summary of all the endpoint expressions

	Kinematic Endpoint	Mass conditions
m_{qqll}	$m_{qqll}^{2\max} = \dfrac{(m_{\tilde{g}}^2 - m_{\tilde{q}}^2)(m_{\tilde{q}}^2 - m_{\tilde{\chi}_1}^2)}{m_{\tilde{q}}^2}$	$m_{\tilde{q}}^2 \le m_{\tilde{\chi}_1} m_{\tilde{g}}$
	$m_{qqll}^{2\max} = (m_{\tilde{q}}^2 - m_{\tilde{\chi}_2}^2)(\dfrac{m_{\tilde{g}}^2 m_{\tilde{\chi}_2}^2 - m_{\tilde{\chi}_1}^2 m_{\tilde{q}}^2}{m_{\tilde{q}}^2 m_{\tilde{\chi}_2}^2})$	$m_{\tilde{q}}^2 m_{\tilde{\chi}_1} \ge m_{\tilde{\chi}_2}^2 m_{\tilde{g}}$
	$m_{qqll}^{2\max} = (m_g - m_{\tilde{\chi}_1})^2$	Otherwise
$m_{qll(high)}$	$m_{qll(high)}^{\max} = \max\{m_{q_n ll}^{\max}, m_{q_f ll}^{\max}\}$	
$m_{qll(low)}$	$m_{qll(low)}^{\max} = \min\{m_{q_n ll}^{\max}, m_{q_f ll}^{\max}\}$	
$m_{q_{far}ll}$	$(m_{q_f ll}^2)^{edge} = (m_{\tilde{q}} - m_{\tilde{\chi}_1})^2$	$m_{\tilde{\chi}_2}^2 \ge m_{\tilde{q}} m_{\tilde{\chi}_1}$
	$(m_{q_f ll}^2)^{edge} = (m_{\tilde{q}}^2 - m_{\tilde{\chi}_2}^2)(m_{\tilde{\chi}_2}^2 - m_{\tilde{\chi}_1}^2)/m_{\tilde{\chi}_2}^2$	Otherwise
$m_{q_{near}ll}$	$(m_{q_n ll}^2)^{edge} = (\sqrt{m_{\tilde{\chi}_2}^2 + m_{\tilde{g}}^2 - m_{\tilde{q}}^2} - m_{\tilde{\chi}_1})^2$	$m_{\tilde{\chi}_2}^2 \ge m_{\tilde{\chi}_1}\sqrt{m_{\tilde{\chi}_2}^2 + m_{\tilde{g}}^2 - m_{\tilde{q}}^2}$
	$(m_{q_n ll}^2)^{edge} = (m_{\tilde{g}}^2 - m_{\tilde{q}}^2)(m_{\chi_2}^2 - m_{\chi_1}^2)/m_{\chi_2}^2$	Otherwise
$m_{qql(high)}$	$(m_{qql(high)}^{\max})^2 = (\dfrac{(m_{\tilde{g}}^2 - m_{\tilde{\chi}_2}^2)(m_{\tilde{\chi}_2}^2 - m_{\tilde{\chi}_1}^2)}{m_{\tilde{\chi}_2}^2})$	$m_{\tilde{\chi}_2}^2 \ge m_{\tilde{g}} m_{\tilde{\chi}_1}$
	$(m_{qql(high)}^{\max})^2 = (\dfrac{(m_{\tilde{g}}^2 - m_{\tilde{q}}^2)(m_{\tilde{q}}^2 - m_{\tilde{\chi}_1}^2)}{m_{\tilde{q}}^2})$	$m_{\tilde{q}}^2 \le m_{\tilde{g}} m_{\tilde{\chi}_1}$
	$(m_{qql(high)}^{\max})^2 = (m_{\tilde{q}}^2 - m_{\tilde{\chi}_2}^2)(\dfrac{m_{\tilde{g}}^2 m_{\tilde{\chi}_2}^2 - m_{\tilde{q}}^2 m_{\tilde{\chi}_1}^2}{m_{\tilde{q}}^2 m_{\tilde{\chi}_2}^2})$	$m_{\tilde{q}}^2 m_{\tilde{\chi}_1} \ge m_{\tilde{g}} m_{\tilde{\chi}_2}^2$
	$(m_{qql(high)}^{\max})^2 = (m_{\tilde{g}} - m_{\tilde{\chi}_1})^2$	Otherwise
$m_{qql(low)}$	Incomplete	
	$(m_{qql(low)}^{\max})^2 = \max\{A, B\}$	$m_{\tilde{\chi}_2}^2 \ge m_{\tilde{g}} x$
	$(m_{qql(low)}^{\max})^2 = \max\{A, C\}$	$m_{\tilde{q}}^2 \le m_{\tilde{g}} x$
	$(m_{qql(low)}^{\max})^2 = \max\{A, D\}$	$m_{\tilde{q}}^2 x \ge m_{\tilde{g}} m_{\tilde{\chi}_2}^2$
	$(m_{qql(low)}^{\max})^2 = \max\{A, E\}$	Otherwise

	$A = m_{\tilde{\chi}_2} m_{\tilde{\chi}_1} + m_{\tilde{g}}^2 - (m_{\tilde{\chi}_1} + m_{\tilde{\chi}_2})(\frac{m_{\tilde{g}}^2 m_{\tilde{\chi}_2}^2 + m_{\tilde{q}}^4}{2m_{\tilde{q}}^2 m_{\tilde{\chi}_2}})$ $B = (\frac{(m_{\tilde{g}}^2 - m_{\tilde{\chi}_2}^2)(m_{\tilde{\chi}_2}^2 - x^2)}{m_{\tilde{\chi}_2}^2})$ $C = (\frac{(m_{\tilde{g}}^2 - m_{\tilde{q}}^2)(m_{\tilde{q}}^2 - x^2)}{m_{\tilde{q}}^2})$ $D = (m_{\tilde{q}}^2 - m_{\tilde{\chi}_2}^2)(\frac{m_{\tilde{g}}^2 m_{\tilde{\chi}_2}^2 - m_{\tilde{q}}^2 x^2}{m_{\tilde{q}}^2 m_{\tilde{\chi}_2}^2})$ $E = (m_{\tilde{g}} - x)^2$	$x = \sqrt{\frac{m_{\tilde{\chi}_2}^2 + m_{\tilde{\chi}_1}^2}{2}}$
$m_{ql(huge)}$	$m_{ql(HUGE)}^{\max} = \max\{m_{q_{near}l(high)}^{\max}, m_{q_{far}l(high)}^{\max}\}$	
$m_{ql(large)}$	$m_{ql(LARGE)}^{\max} = \max\{m_{q_>l(low)}^{\max}, m_{q_<l(high)}^{\max}\}$	
$m_{ql(little)}$	*	
$m_{ql(tiny)}$	$m_{ql(TINY)}^{\max} = \min\{m_{q_{near}l(low)}^{\max}, m_{q_{far}l(low)}^{\max}\}$	
$m_{q_{far}l(high)}$	$(m_{q_{far}l(high)}^{\max})^2 = (\frac{(m_{\tilde{q}}^2 - m_{\tilde{\chi}_2}^2)(m_{\tilde{\chi}_2}^2 - m_{\tilde{\chi}_1}^2)}{m_{\tilde{\chi}_2}^2})$ ✓	
$m_{q_{far}l(low)}$	$(m_{q_{far}l(low)}^{\max})^2 = (\frac{(m_{\tilde{q}}^2 - m_{\tilde{\chi}_2}^2)(m_{\tilde{\chi}_2}^2 - m_{\tilde{\chi}_1}^2)}{2m_{\tilde{\chi}_2}^2})$ ✓	
$m_{q_{near}l(high)}$	$(m_{q_{near}l(high)}^{\max})^2 = (\frac{(m_{\tilde{g}}^2 - m_{\tilde{q}}^2)(m_{\tilde{\chi}_2}^2 - m_{\tilde{\chi}_1}^2)}{m_{\tilde{\chi}_2}^2})$	
$m_{q_{near}l(low)}$	$(m_{q_{near}l(low)}^{\max})^2 = (\frac{(m_{\tilde{g}}^2 - m_{\tilde{q}}^2)(m_{\tilde{\chi}_2}^2 - m_{\tilde{\chi}_1}^2)}{2m_{\tilde{\chi}_2}^2})$	
m_{qq}	$(m_{qq}^2)^{\max} = (m_{\tilde{g}}^2 - m_{\tilde{q}}^2)(m_{\tilde{q}}^2 - m_{\tilde{\chi}_2}^2)/m_{\tilde{q}}^2$	
m_{ll}	$(m_{ll}^2)^{\max} = (m_{\tilde{\chi}_2} - m_{\tilde{\chi}_1})^2$ ✓	

The subscripts > and < stand for the quark with the higher and lower endpoint respectively.

Analysis

Mass distributions and ratio plots

For the endpoint method to be useful, the edge of the mass distribution must have a clearly defined endpoint. If the edge becomes concave at the higher vales then the endpoint will be underestimated by the simulation and experiment. The more phase space in the vicinity of the endpoint, the more likely it is for a decay to take place with an invariant mass close to the endpoint value.

In reality the distributions will differ from those produced in this study, as only decay phase space has been used without the associated matrix elements. This ignores possible spin correlations between leptons and/or quarks in addition to other detector effects and background. However for the purposes of this study, simply to test the derived endpoint positions, use of the basic shapes is adequate.

One should also keep in mind that quark resolution at ATLAS will be much poorer than lepton resolution due to all the QCD background and jets from the proton collisions. ATLAS is unable to distinguish between types of quark as they all produce jets, other than the b quark which has a much shorter lifetime than the others. Therefore, in general, endpoints with fewer or no quarks will be more useful than quark endpoints.

The invariant mass distributions were generated for each mass region that produces a different endpoint, to investigate how the distributions vary with the SUSY masses. Histograms were also produced to show the ratio of simulation to theoretical endpoint value for 1000 randomly generated mass sets. For the histograms reproduced here, one million events were generated for each mass region. Mass distributions with an almost vertical edge are expected to have ratios very near one and sloping edges resulting in a slightly poorer correlation. If any ratios are above one then the theoretical value is incorrect, at least for a certain mass region.

As expected, the m_{qq} and m_{ll} distributions are zero at the origin increasing linearly up to the maximum, giving a clean cut-off as the edge, (figure 7(a)). This is because they are constructed from two nearest neighbours in the decay chain and so the uniformly distributed $\cos\theta$ is the only variable to enter the invariant mass squared expression, where θ is the angle between the two particles. As m_{ll}^2 and m_{qq}^2 have uniform distributions, the m_{qq} and m_{ll} distributions are linear, resulting in very accurate endpoint identification (figure 7(b)).

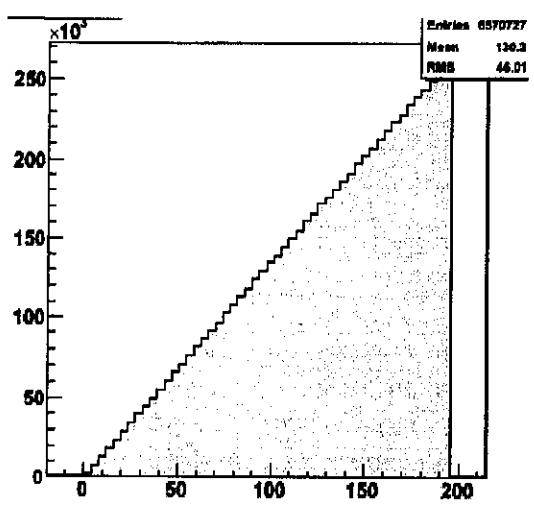

Figure 7(a) Invariant mass distribution of m_{qq}

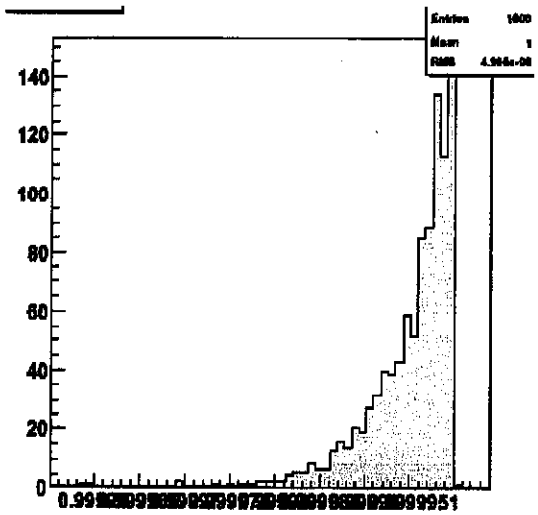

Figure 7(b) Ratio histogram shows mean ratio of one between simulation and theoretical values for $m_{qq}^{\max}$

In all mass regions, the $m_{q_{far}ll}$ distribution also drops off quite sharply but the edge of the $m_{q_{near}ll}$ distribution slopes gently towards zero, (figure 8 (a), (b)). The high and low qll distributions, in the vicinity of the endpoint, are found to have similar shapes to the appropriate near or far edge. The ratio histograms reflect these shapes as the correlation between the simulation and theoretical endpoints is slightly better for the $m_{q_{far}ll}$ than the $m_{q_{near}ll}$ endpoint. The far quark histogram peaks nearer one and has slightly higher mean ratio than the near quark, (figure 8(c) and (d)). The correlation is also better for the qll(low) endpoints than for the qll(high) endpoints, suggesting that the $m_{q_{far}ll}$ endpoint is the lower endpoint more often, (figure 8(e) and (f)).

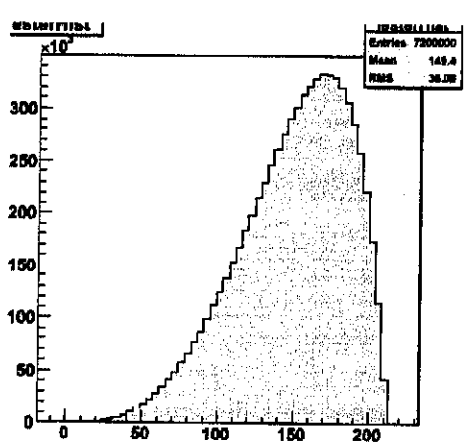

Figure 8 (a)

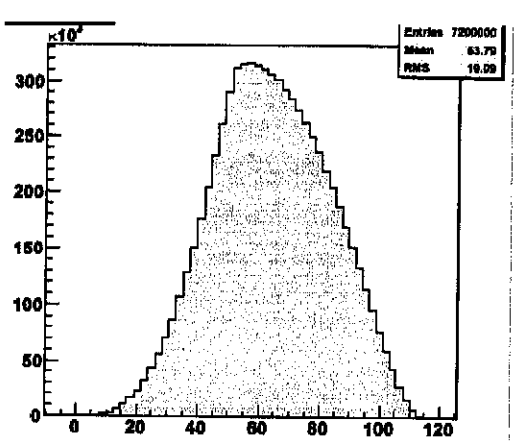

Figure 8(b)

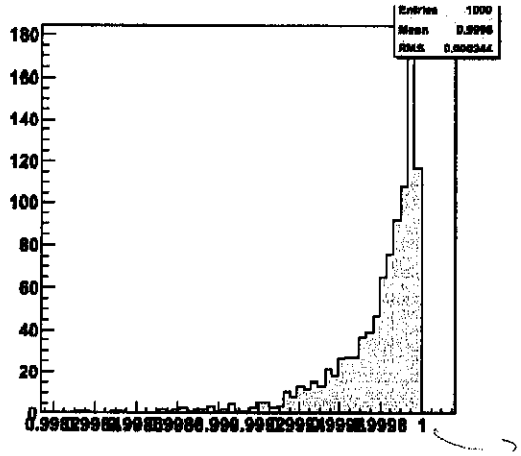

Figure 8(c)

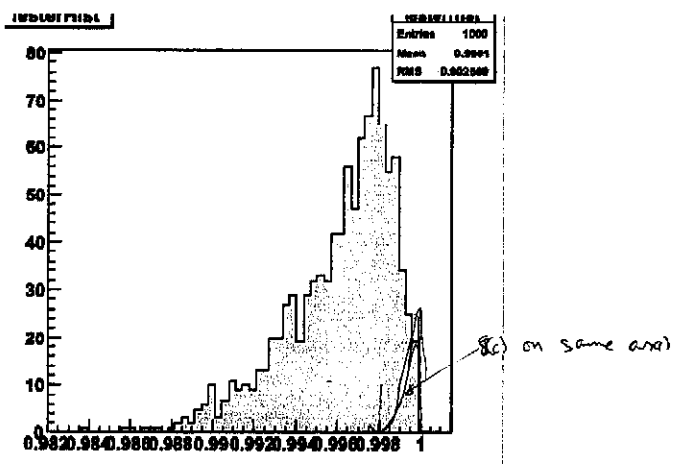

Figure 8(d)

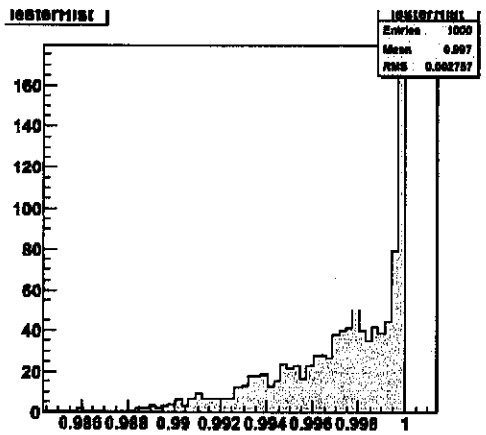

Figure 8(e)

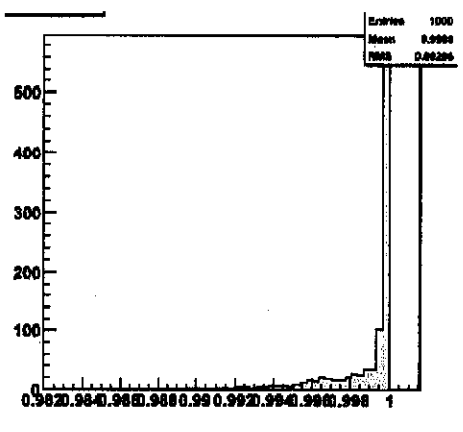

Figure 8(f)

Figure 8; (a) Invariant mass distribution for $m_{q_{far}ll}$, (b) Invariant mass distribution for $m_{q_{near}ll}$, Ratio histograms between simulation and theoretical endpoint values for (c) $m_{q_{far}ll}$, (d) $m_{q_{near}ll}$, (e) $m_{qll(high)}$ and (f) $m_{qll(low)}$ (Note different scales along both axes)

The m_{qqll} invariant mass distribution varies between mass regions in a more obvious way than the other distributions, (figures 9(a) (b) and (c)). All three regions show quite a sharp edge but each have a little 'foot' which could lead to misidentification of the endpoint without high enough statistics. The resulting ratio plot (figure 9(d)) peaks very near one, showing good correlation between the theoretical and simulation endpoint values.

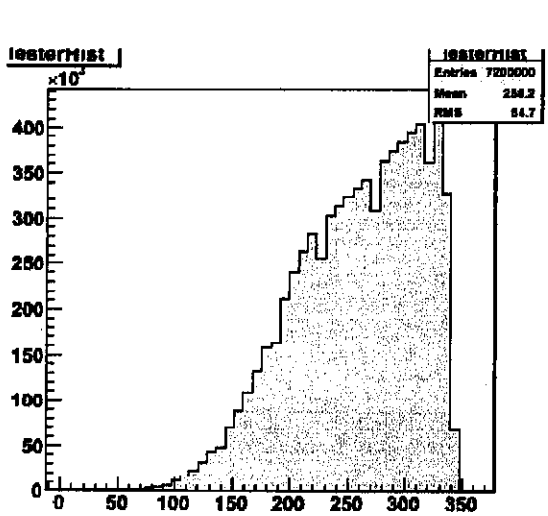

Figure 9 (a)

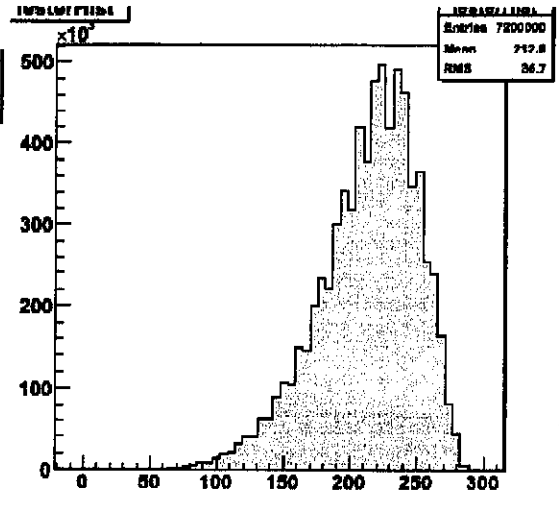

Figure 9(b)

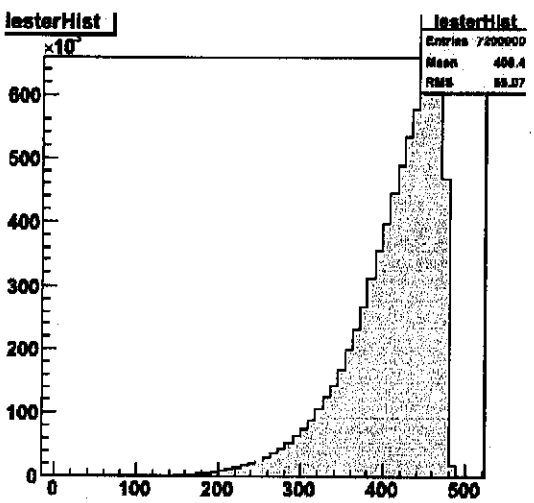

Figure 9 (c)

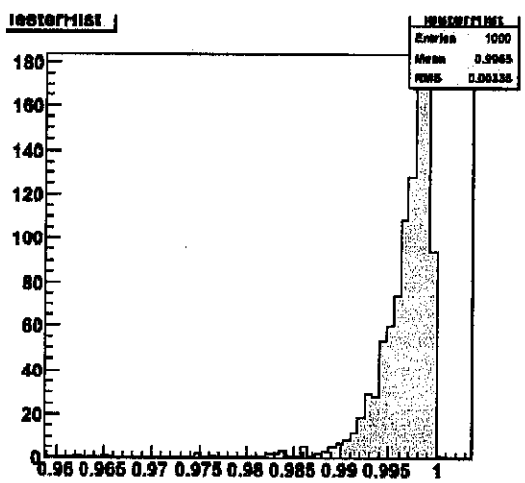

Figure 9 (d)

Figure 9 (a)-(c) Invariant mass distributions for m_{qqll}; (a) for the mass region $m_{\tilde{q}}^2 \leq m_{\tilde{\chi}_1} m_{\tilde{g}}$ (b) $m_{\tilde{q}}^2 m_{\tilde{\chi}_1} \geq m_{\tilde{\chi}_2}^2 m_{\tilde{g}}$, (c) remaining mass regions, (d) Histogram showing ratios of simulation to theoretical endpoint values.

In contrast, none of the m_{ql} distributions have sharp edges, with particularly sloping edges associated with the near quark, (figure 10 (a) and (b)). These are mirrored by the observable distributions. As a result the ratio plots have a more Gaussian distribution, peaking near the mean rather than towards the higher values.

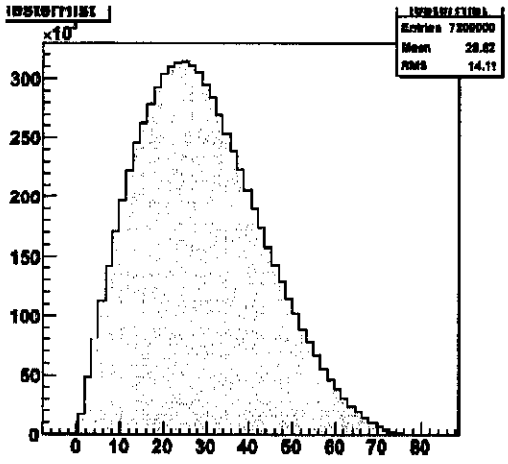

Figure 10 (a) Distribution of $m_{q_{near}l(low)}$

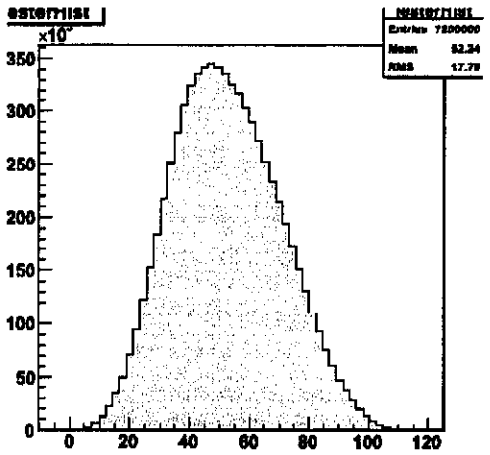

Figure 10 (b) Distribution of $m_{q_{near}l(high)}$

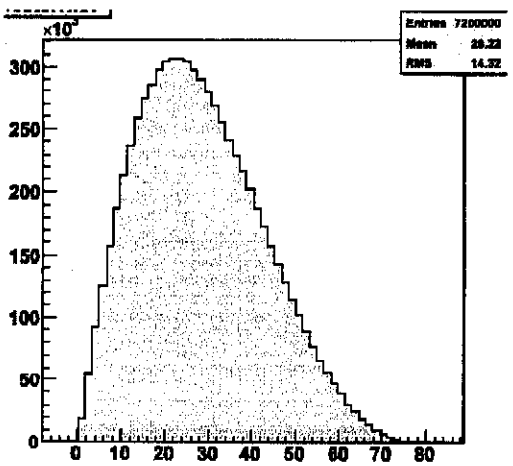

Figure 10(b) Distribution of $m_{ql(TINY)}$

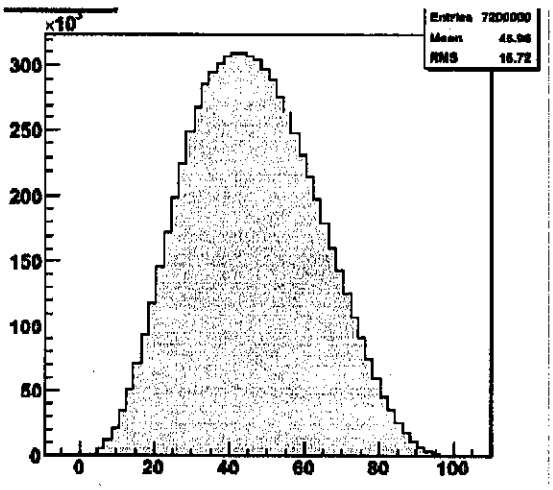

Figure 10 (c) Distribution of $m_{ql(LITTLE)}$

When the theoretical value of $m^{max}_{ql(LITTLE)}$ was set to be the third largest of the near and far m_{ql} endpoints, no ratios above one were found, but it was clear that the correlation could be improved upon. The mass distribution shape for $m_{ql(LITTLE)}$, (figure 10(c)) gives no indication that the ratios should be much lower than for huge, large and tiny, but some reach as low as 0.8 (figure 10 (f)). When comparing the simulation near and far m_{ql} endpoints in descending order, with the simulation huge, large, little and tiny m_{ql} endpoints, the ratio was found to be exactly one for huge, large and tiny but not for little. This showed that $m^{max}_{ql(LITTLE)}$ is not always directly related to the far and near quark unobservable m_{ql} endpoints, unlike the other three observables.

Worth a question?

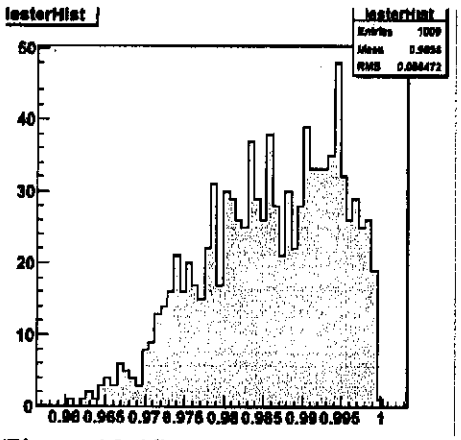

Figure 10 (d)

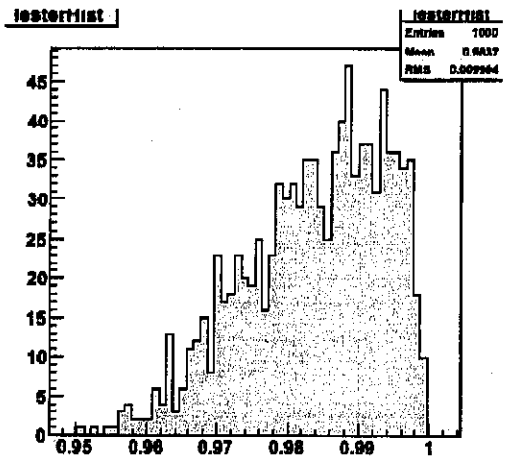

Figure 10 (e)

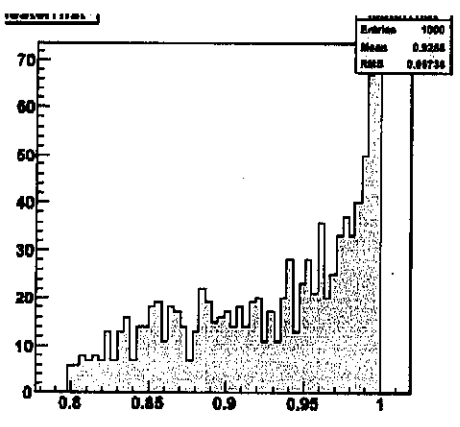

Figure 10 (f)

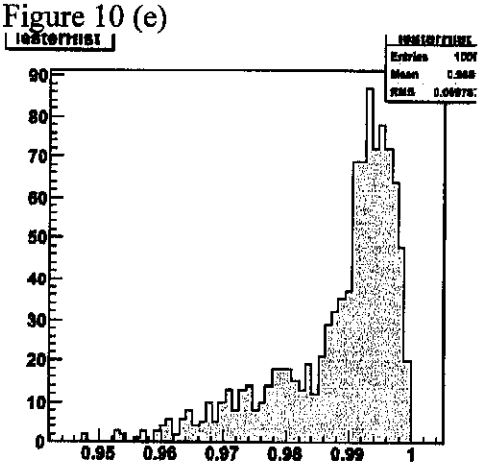

Figure 10 (g)

Figure 10; Ratio histograms between simulation and theoretical endpoint values for (d) $m^{\max}_{ql(HUGE)}$ (e) $m^{\max}_{ql(LARGE)}$ (f) $m^{\max}_{ql(LITTLE)}$ and (g) $m^{\max}_{ql(TINY)}$

The distributions for both $m_{qql(high)}$ and $m_{qql(low)}$ have a sharp edge although once again there is a small foot at the endpoint, (figure 11 (a) and (b)). Figure 11 (c) shows good correlation for $m_{qql(high)}$. However the ratio plot generated using just the initial four endpoints derived for $m_{qql(low)}$ shows that the theoretical positions were too low in many mass regions, (figure 11 (d)). This was improved upon with the addition of the fifth endpoint. Unfortunately, with high enough statistics, there are still some ratios just above one, (figure 11 (e)).

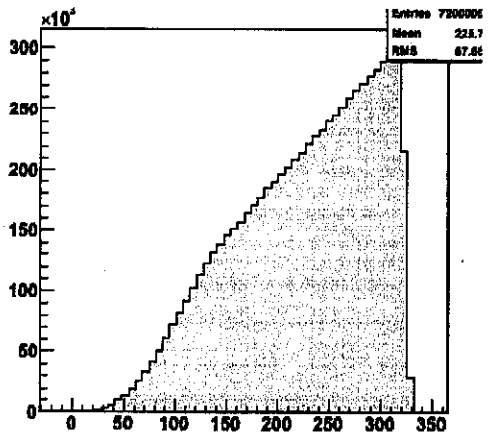

Figure 11 (a) Distribution of $m_{qql(low)}$

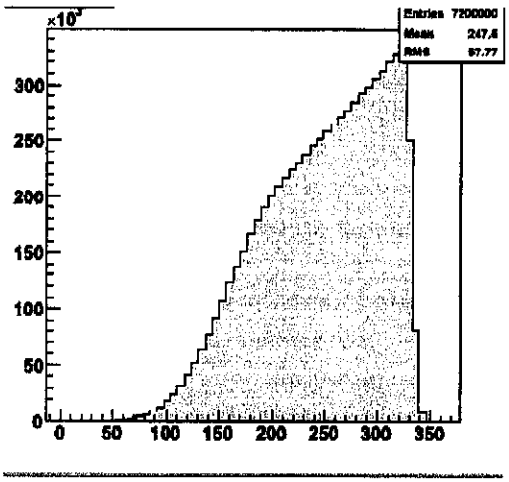

Figure 11 (b) Distribution of $m_{qql(high)}$

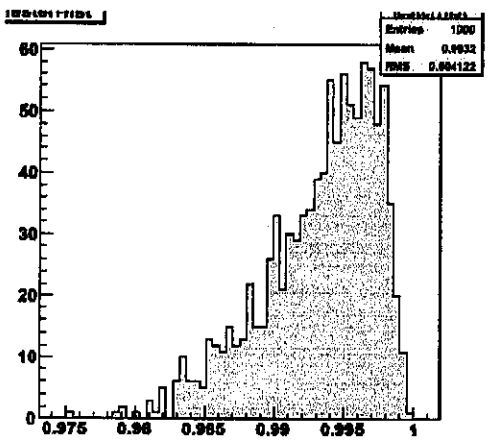

Figure 11 (c) Ratio plot for $m^{\max}_{qql(high)}$

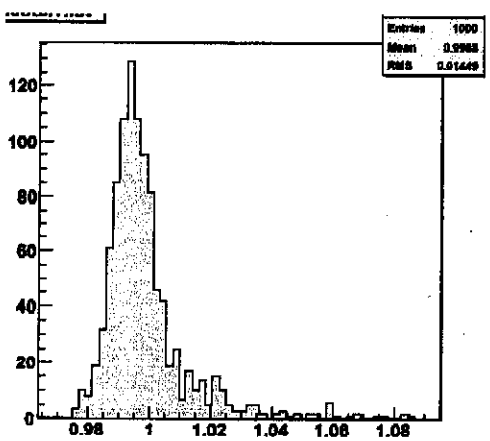

Figure 11 (d) Initial ratio plot for $m^{\max}_{qql(low)}$

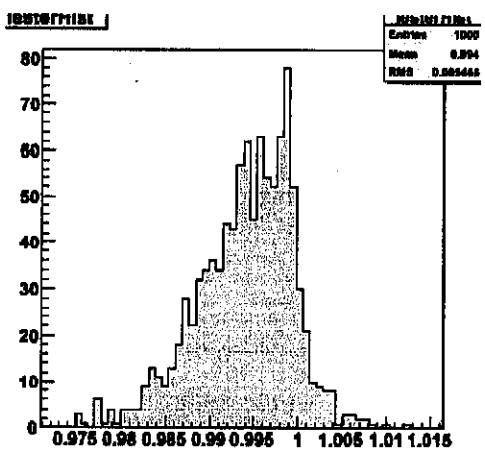

Figure 11 (e) Ratio plot for $m^{\max}_{qql(low)}$ with fifth endpoint expression included

Other than for $m_{ql(LITTLE)}^{\max}$ and $m_{qql(low)}^{\max}$, all the ratio plots showed that the simulated endpoints agree very well with the theoretical values and most importantly that the agreement improves with increasing statistics. The mass distributions do not vary greatly between mass regions so a general shape can be assumed for each edge.

Mass reconstruction

Extending the chain in [2] to include a gluino at the head has increased the number of observable kinematic endpoints from four to eleven and therefore the constraints on the SUSY masses are much improved. However some of the endpoints still have very similar expressions; m_{qqll} has three possible endpoints, all of which are at the same position as $m_{qql(high)}^{\max}$ in particular mass regions. $m_{ql(high)}^{\max}$ coincides with $m_{qll}^{\max}$ for each quark in some mass regions, with $m_{ql(low)}^{\max}$ differing by a factor of $\sqrt{2}$ only. Despite this, there are still enough independent expressions in each mass region to evaluate the SUSY masses.

It should be noted that the $m_{\tilde{q}}$ will be a mixture of all the squark masses that the gluino can decay into, and so will represent the squark mass scale rather than a particular mass. However, for models such as NUHM which has a relatively light gluino only stop and sbottom squarks will be involved.

Conclusions

If events at the LHC are to extend usefully the Standard Model, then it is vital to establish methods now to interpret the resulting data. Our capability to measure the sparticle masses will play an essential part in validating or disproving supersymmetry and will be a key component to gaining a deeper understanding of it.

In this study, the endpoint method of calculating sparticle masses has been applied to the decay chain in figure 5 consisting of two two-body decays followed by a three-body decay. This is an extension of the decay considered in [2] by the addition of a gluino at the head of the chain, resulting in eleven endpoints. Throughout the derivations of these endpoints, the mass hierarchy condition $m_{\tilde{g}} > m_{\tilde{q}} > m_{\tilde{\chi}_2} > m_{\tilde{\chi}_1}$ was assumed. A montecarlo event generator was used to generate invariant mass distributions and to test the derived endpoint expressions for a large range of sparticle mass combinations. The generated endpoints, which are the highest invariant masses produced in the simulation, were compared with the theoretical predictions and were found to correlate extremely well for all but two of the endpoints in each mass region. Further work must be done to establish the correct expressions for $m_{ql(LITTLE)}^{\max}$ and $m_{qql(low)}^{\max}$.

ideas ?

Although some of the endpoints are found to have coincident expressions in certain mass regions, it is always possible to calculate the sparticle masses of this decay chain, assuming the chain is identified correctly and that ATLAS can locate the endpoints despite all the background and detector effects. Therefore this endpoint method can be applied to any supersymmetry model in which this event occurs, no matter how the sparticle masses relate to one another, other than the general hierarchy.

unless very degenerate spine leads to soft emitted particles?

Appendix A

The qll endpoints

Near and Far

Derivation of the $q_{far}ll$ endpoint can be found in [2]. The $q_{near}ll$ edge is derived in a similar manner. The two leptons are treated as an effective particle, with a mass equal to their invariant mass. This enables the decay to be simplified to a two-body decay. In [2] it was found that $m_{ll}^{\max} = (m_{\tilde{\chi}_2} - m_{\chi_1})$, so the effective particle can have a mass varying from zero, when the leptons are collinear, to $m_{ll}^{\max}$, when they are back to back in the $\tilde{\chi}_2^0$ rest frame . Therefore we define

$$m_{ll}^2 = \lambda(m_{\tilde{\chi}_2} - m_{\chi_1})^2 \qquad \lambda \in [0,1] \qquad \text{A1}$$

In order to maximise $m_{q_{near}ll}$, the near quark is set back to back with the ll effective particle in the squark rest frame. Tthe angle ϕ, between the far quark and the ll effective particle in the $\tilde{\chi}_2^0$ rest frame must also be taken into account.

Hence, by applying [h]

$$m_{q_{near}ll}^2 = m_{ll}^2 + 2Q_{near}^{\tilde{q}}(E_L^{\tilde{q}} + L^{\tilde{q}})$$

where the superscript refers to the rest frame, in this case the squark, Q is the quark momentum and $E_L = \sqrt{m_{ll}^2 + L^2}$ refers to the energy of the effective particle with momentum L.

Using [d] and [e]

$$Q_{far}^{\tilde{q}} = \frac{m_{\tilde{q}}^2 - m_{\tilde{\chi}_2}^2}{2m_{\tilde{q}}} \qquad \text{A2} \qquad\qquad Q_{near}^{\tilde{q}} = \frac{m_{\tilde{g}}^2 - m_{\tilde{q}}^2}{2m_{\tilde{q}}} \qquad \text{A3}$$

The energy and momentum of the lepton pair must first be calculated in the rest frame of $\tilde{\chi}_2^0$ and then lorentz boosted to the squark rest frame.

$$L^{\tilde{\chi}_2} = \frac{\sqrt{m_{ll}^4 + m_{\tilde{\chi}_2}^4 + m_{\tilde{\chi}_1}^4 - 2(m_{ll}^2 m_{\tilde{\chi}_2}^2 + m_{ll}^2 m_{\tilde{\chi}_1}^2 + m_{\tilde{\chi}_2}^2 m_{\tilde{\chi}_1}^2)}}{2m_{\tilde{\chi}_2}} \quad \text{A4}$$

$$E_L^{\tilde{\chi}_2} = \sqrt{m_{ll}^2 + (L^{\tilde{\chi}_2})^2} = \frac{m_{ll}^2 + m_{\tilde{\chi}_2}^2 - m_{\tilde{\chi}_1}^2}{2m_{\tilde{\chi}_2}} \qquad \text{A5}$$

$$E_{\tilde{\chi}_2}^{\tilde{q}} = \sqrt{m_{\tilde{\chi}_2}^2 + (Q_{far}^{\tilde{q}})^2} \qquad \text{A6}$$

$$m_{q_{near}ll}^2 = m_{ll}^2 + 2\frac{Q_{near}^{\tilde{q}}}{m_{\tilde{\chi}_2}}(E_L^{\tilde{\chi}_2} + L^{\tilde{\chi}_2})(E_{\tilde{\chi}_2}^{\tilde{q}} - Q_{far}^{\tilde{q}}\cos\phi)$$

This is maximised when ϕ is 180 degrees, meaning the far quark is back to back with the ll effective particle in the $\tilde{\chi}_2^0$ rest frame. This could also produce the $m_{q_{far}ll}$ maximum, depending on the value of m_{ll}, that is the value of λ in A1, which is now evaluated to find the true maximum of A7.

$$m^2_{q_{near}ll} = m^2_{ll} + \frac{m^2_{\tilde{g}} - m^2_{\tilde{q}}}{2m^2_{\tilde{\chi}_2}}[m^2_{ll} + m^2_{\chi_2} - m^2_{\chi_1} + \sqrt{(m^2_{\chi_2} + m^2_{\chi_1} - m^2_{ll})^2 - 4m^2_{\chi_2}m^2_{\chi_1}}] \quad \text{A7}$$

There are three cases to consider; when λ is zero, one, or when it has a value in-between.

$0 < \lambda < 1$

Differentiating A7 with respect to m^2_{ll} (equivalent to differentiating with respect to λ), setting the result equal to zero and solving for m_{ll} gives

$$m^2_{ll} = m^2_{\chi_2} + m^2_{\chi_1} - \sqrt{\frac{m^2_{\chi_1}}{m^2_{\tilde{g}} + m^2_{\chi_2} - m^2_{\tilde{q}}}(m^2_{\tilde{g}} + 2m^2_{\chi_2} - m^2_{\tilde{q}})} \qquad \text{A8}$$

This maximises A7 for this range of λ. Substituting A8 back into A7 gives

$$m^{\max(\lambda)}_{q_{near}ll} = (\sqrt{m^2_{\tilde{g}} + m^2_{\chi_2} - m^2_{\tilde{q}}} - m_{\tilde{\chi}_1}) \qquad \text{A9}$$

The $\lambda > 0$ ($m_{ll} > 0$) bound implies the following condition

$$m^2_{\tilde{\chi}_2} \geq m_{\tilde{\chi}_1}\sqrt{m^2_{\tilde{\chi}_2} + m^2_{\tilde{g}} - m^2_{\tilde{q}}} \qquad \text{A10}$$

When this is not satisfied, the $\lambda = 0$ expression must be found. Setting m_{ll} to zero in A7 yields;

$$(m^{\max(0)}_{q_{near}ll})^2 = \frac{(m^2_{\tilde{g}} - m^2_{\tilde{q}})(m^2_{\chi_2} - m^2_{\chi_1})}{m^2_{\chi_2}}$$

It is found that λ is always less than one so only these two expressions are required. In those mass regions where the invariant mass is maximised by having $\lambda = 0$, both $m_{q_{far}ll}$ and $m_{q_{near}ll}$ are maximised. However, the equivalent of A8 for the far quark is

$$m^2_{ll} = m^2_{\chi_2} + m^2_{\chi_1} - \sqrt{\frac{m^2_{\chi_1}}{m^2_{\tilde{q}}}(m^2_{\chi_2} + m^2_{\tilde{q}})}$$

so $m_{q_{far}ll}$ is not necessarily at its absolute maximum when $m_{q_{near}ll}$ is.

Summary

$m_{q_{far}ll}$	$(m^2_{q_{fll}})^{edge} = (m_{\tilde{q}} - m_{\tilde{\chi}_1})^2$	$m^2_{\tilde{\chi}_2} \geq m_{\tilde{q}} m_{\tilde{\chi}_1}$
	$(m^2_{q_{fll}})^{edge} = (m^2_{\tilde{q}} - m^2_{\tilde{\chi}_2})(m^2_{\tilde{\chi}_2} - m^2_{\tilde{\chi}_1}) / m^2_{\tilde{\chi}_2}$	Otherwise
$m_{q_{near}ll}$	$(m^2_{q_{nll}})^{edge} = (\sqrt{m^2_{\tilde{\chi}_2} + m^2_{\tilde{g}} - m^2_{\tilde{q}}} - m_{\tilde{\chi}_1})^2$	$m^2_{\tilde{\chi}_2} \geq m_{\tilde{\chi}_1} \sqrt{m^2_{\tilde{\chi}_2} + m^2_{\tilde{g}} - m^2_{\tilde{q}}}$
	$(m^2_{q_{nll}})^{edge} = (m^2_{\tilde{g}} - m^2_{\tilde{q}})(m^2_{\chi_2} - m^2_{\chi_1}) / m^2_{\chi_2}$	Otherwise

The qqll edge

This derivation uses $q_{far}ll$ as an effective particle, so the derivation can be done modelling the decay as a single two-body decay as shown in figure 6. Using A5

$$m^2_{qqll} = m^2_{q_{far}ll} + 2Q^{\tilde{q}}_{near}(E^{\tilde{q}}_{q_{far}ll} + P^{\tilde{q}})$$

The effective particle momentum is,

$$P^{\tilde{q}} = \sqrt{\frac{m^4_{\tilde{q}} + m^4_{q_{far}ll} + m^4_{\chi_1} - 2(m^2_{\chi_1} m^2_{q_{far}ll} + m^2_{\chi_1} m^2_{\tilde{q}} + m^2_{\tilde{q}} m^2_{q_{far}ll})}{4m^2_{\tilde{q}}}}$$

with energy

$$E^{\tilde{q}}_{qll} = \sqrt{m^2_{q_{far}ll} + (P^{\tilde{q}})^2} = \frac{m^2_{q_{far}ll} + m^2_{\tilde{q}} - m^2_{\tilde{\chi}_1}}{2m_{\tilde{q}}}$$

Substituting in these values together with A3 gives,

$$m^2_{qqll} = m^2_{q_{far}ll} + \frac{m^2_{\tilde{g}} - m^2_{\tilde{q}}}{2m^2_{\tilde{q}}}[m^2_{q_{far}ll} + m^2_{\tilde{q}} - m^2_{\chi_1} + \sqrt{(m^2_{\tilde{q}} + m^2_{\chi_1} - m^2_{q_{far}ll})^2 - 4m^2_{\tilde{q}} m^2_{\chi_1}}] \quad \text{A11}$$

This is the maximum for a given value of $m^2_{q_{far}ll}$, but to find the true maximum $m^2_{q_{far}ll}$ must be varied between zero and its maximum value.

$m^2_{q_{far}ll} = \lambda (m^{max}_{q_{far}ll})^2 \qquad \lambda \in [0,1]$

how many values does this have?

To find the value of A11 when λ is between extreme values, A11 is differentiated with respect to λ and set to zero. Solving this for $m^2_{q_{far}ll}$ gives

$$m^2_{q_{far}ll} = m^2_{\tilde{q}} + m^2_{\chi_1} - \frac{m_{\chi_1}}{m_{\tilde{g}}}(m^2_{\tilde{g}} + m^2_{\tilde{q}}) \qquad \text{A12}$$

Substituting A12 back into A11 gives

$$m_{qqll} = (m_g - m_{\tilde{\chi}_1})$$

The $\lambda > 0$ ($m_{ll} > 0$) bound holds if $m_{\tilde{q}}^2 \geq m_{\tilde{\chi}_1} m_{\tilde{g}}$. When this is invalid, an alternative endpoint position is needed. This is found by setting $m_{q_{far}ll}^2$ to zero in A11 to give

$$m_{qqll}^2 = \frac{(m_{\tilde{g}}^2 - m_{\tilde{q}}^2)(m_{\tilde{q}}^2 - m_{\tilde{\chi}_1}^2)}{m_{\tilde{q}}^2}$$

Turning to the other extreme, $\lambda = 1$, sets $m_{q_{far}ll}^2$ to its maximum value. However it was found in [2] that

$$m_{q_{far}ll}^{\max} = (m_{\tilde{q}} - m_{\tilde{\chi}_1}) \text{ iff } m_{\tilde{\chi}_2}^2 \geq m_{\tilde{q}} m_{\tilde{\chi}_1} \qquad \text{A13}$$

$$(m_{q_f ll}^2)^{edge} = (m_{\tilde{q}}^2 - m_{\tilde{\chi}_2}^2)(m_{\tilde{\chi}_2}^2 - m_{\tilde{\chi}_1}^2)/m_{\tilde{\chi}_2}^2 \quad \text{otherwise} \qquad \text{A14}$$

Each of these must be considered separately.

It can be ascertained that under no conditions will $m_{q_{far}ll}^2$ have the value of A13 as the $\lambda<1$ boundary always holds for this case. This is not true for A14, in which case the $\lambda<1$ boundary is

$$m_{q_{far}ll}^2 = m_{\tilde{q}}^2 + m_{\chi_1}^2 - \frac{m_{\chi_1}}{m_{\tilde{g}}}(m_{\tilde{g}}^2 + m_{\tilde{q}}^2) < (m_{\tilde{q}}^2 - m_{\tilde{\chi}_2}^2)(m_{\tilde{\chi}_2}^2 - m_{\tilde{\chi}_1}^2)/m_{\tilde{\chi}_2}^2$$

yielding $\qquad m_{\tilde{q}}^2 m_{\tilde{\chi}_1} \leq m_{\tilde{\chi}_2}^2 m_{\tilde{g}}$

When this is not valid, $\lambda=1$ and a third solution is found by substituting A14 into A11 producing;

$$(m_{qqll}^{\max})^2 = (m_{\tilde{q}}^2 - m_{\tilde{\chi}_2}^2)\left(\frac{m_{\tilde{g}}^2 m_{\tilde{\chi}_2}^2 - m_{\tilde{\chi}_1}^2 m_{\tilde{q}}^2}{m_{\tilde{q}}^2 m_{\tilde{\chi}_2}^2}\right)$$

Summary

$(m_{qqll}^{\max})^2 = \frac{(m_{\tilde{g}}^2 - m_{\tilde{q}}^2)(m_{\tilde{q}}^2 - m_{\tilde{\chi}_1}^2)}{m_{\tilde{q}}^2}$	$m_{\tilde{q}}^2 \leq m_{\tilde{\chi}_1} m_{\tilde{g}}$
$(m_{qqll}^{\max})^2 = (m_{\tilde{q}}^2 - m_{\tilde{\chi}_2}^2)\left(\frac{m_{\tilde{g}}^2 m_{\tilde{\chi}_2}^2 - m_{\tilde{\chi}_1}^2 m_{\tilde{q}}^2}{m_{\tilde{q}}^2 m_{\tilde{\chi}_2}^2}\right)$	$m_{\tilde{q}}^2 m_{\tilde{\chi}_1} \geq m_{\tilde{\chi}_2}^2 m_{\tilde{g}}$
$(m_{qqll}^{\max})^2 = (m_g - m_{\tilde{\chi}_1})^2$	Otherwise

The ql edges

The $m_{q_{far}l}$ endpoints were derived in [2] where it was found that the configuration for $m^{\max}_{q_{far}l(high)}$ is when the far quark is back to back with the lepton in question in the $\tilde{\chi}_2^0$ rest frame. The other lepton is produced at rest and so $\tilde{\chi}_1^0$ is back to back with the moving lepton and therefore parallel to the far quark.

The configuration that maximises the low edge is the same as that for the high edge, apart from that both leptons have identical momentum and both are back to back with the quark.

The same must be true when calculating the $m_{q_{near}l}$ endpoints but now the position of the far quark must also be considered.

Implementing [h] gives

$$(m_{q_{near}l(high)})^2 = 2Q^{\tilde{q}}_{near}\frac{L^{\tilde{\chi}_2}}{m_{\tilde{\chi}_2}}(E^{\tilde{q}}_{\tilde{\chi}_2} - Q^{\tilde{q}}_{far}\cos\phi) \quad \text{A15}$$

With one lepton at rest, the other has momentum L and has been boosted to the squark frame. This is maximised when ϕ=180 degrees, that is when the far quark is back to back with the lepton in the $\tilde{\chi}_2^0$ rest frame.

$$L^{\tilde{\chi}_2} = \frac{(m^2_{\tilde{\chi}_2} - m^2_{\tilde{\chi}_1})}{2m_{\tilde{\chi}_2}}$$

Substituting A2, A3, A6 and the lepton momentum into A15 yields,

$$(m^{\max}_{q_{near}l(high)})^2 = (\frac{(m^2_{\tilde{g}} - m^2_{\tilde{q}})(m^2_{\tilde{\chi}_2} - m^2_{\tilde{\chi}_1})}{m^2_{\tilde{\chi}_2}})$$

In order to calculate the low edge, the lepton momentum is just halved so the final result can immediately be found as

$$(m^{\max}_{q_{near}l(low)})^2 = (\frac{(m^2_{\tilde{g}} - m^2_{\tilde{q}})(m^2_{\tilde{\chi}_2} - m^2_{\tilde{\chi}_1})}{2m^2_{\tilde{\chi}_2}})$$

This means that in order for $m_{q_{near}l}$ to be maximised, $m_{q_{far}l}$ must also be maximised.

Reordering the unobservable endpoints gives, in descending order;

1. $m^{\max}_{q_>l(high)}$
2. $\max\{m^{\max}_{q_>l(low)}, m^{\max}_{q_<l(high)}\}$
3. $\min\{m^{\max}_{q_>l(low)}, m^{\max}_{q_<l(high)}\}$
4. $m^{\max}_{q_<l(low)}$

(Note the subscripts are > and < are used to denote the quark with the higher and lower endpoints, not which is higher or lower for a particular event.) The following discussion shows how this relates to the observable endpoints, high, large, little and tiny.

All the possible decay configurations are divided into four groups as follows.

1. Both quarks are back to back with one lepton, the near quark in the squark rest frame and the far quark in the $\tilde{\chi}^0_2$ rest frame – the other lepton is produced at rest. $m_{ql(HUGE)}$ and $m_{ql(LARGE)}$ equal $m^{\max}_{q_>l(high)}$ and $m^{\max}_{q_<l(high)}$ respectively.
2. As above but leptons have the same momentum and are back to back with the quarks in the respective rest frames. Hence, in this group, both $m_{ql(HUGE)}$ and $m_{ql(LARGE)}$ equal $m^{\max}_{q_>l(low)}$, and $m_{ql(LITTLE)}$ and $m_{ql(TINY)}$ equal $m^{\max}_{q_<l(low)}$.
3. Two configurations, one as groups one and the other group two, but with only the far quark back to back with one or two leptons. The $q_{far}l$(high) or $q_{far}l$(low) invariant masses respectively are at the endpoint positions.
4. All other configurations, not in the above groups.

Note the superscript max is only used to denote an endpoint.

Huge endpoint

It is clear that $m^{\max}_{ql(HUGE)} = m^{\max}_{q_>l(high)}$, which will occur when the event is from group one. If the far quark has the larger momentum then an event in group three, with one lepton at rest, will produce the same $m_{ql(HUGE)}$ as found in group one. No other events can produce a higher $m_{ql(HUGE)}$, so it is simply the highest of the unobservable endpoints.

Large endpoint

$m^{\max}_{ql(LARGE)}$ is the highest of $m^{\max}_{q_<l(high)}$ and $m^{\max}_{q_>l(low)}$ which are the $m_{ql(LARGE)}$ values from group one and two events respectively. Events in group three may place these same endpoints in the large position, if they belong to the far quark. No other event can produce a higher $m_{ql(LARGE)}$. By definition, no $m_{q_<l}$ is higher than $m^{\max}_{q_<l(high)}$ so $m_{ql(LARGE)}$ would have to be a $m_{q_>l}$, but this will never be in the large position and be higher than $m^{\max}_{q_<l(high)}$ and $m^{\max}_{q_>l(low)}$ simultaneously. To be higher than $m^{\max}_{q_<l(high)}$ it must be a $m_{q_>l(low)}$, but this is smaller than $m^{\max}_{q_>l(low)}$ by definition. To be higher than $m^{\max}_{q_>l(low)}$ it must be a $m_{q_>l(high)}$. This cannot be in the large position as it has just been stipulated that it is higher than $m^{\max}_{q_<l(high)}$, so it can not have the second highest m_{ql}. Therefore $m^{\max}_{ql(LARGE)}$ is just the second highest of the unobservable endpoints.

Little endpoint

The most complicated of the four masses is $m^{\max}_{ql(LITTLE)}$. This is because it is unlikely that one of the unobservable endpoints previously evaluated is in the little position. Group one events have a negligible $m_{ql(LITTLE)}$ as the lepton is at rest. Group two will always have $m_{ql(LITTLE)} = m^{\max}_{q_<l(low)}$, which is the smallest of the unobservable endpoints. Group three can also put $m^{\max}_{q_{far}l(low)}$ in the little position, if the far quark has the smaller momentum.

Group four contains an infinite set of configurations, many of which will have a higher $m_{ql(LITTLE)}$ than $m^{\max}_{q_<l(low)}$. Consider an event in group four that is very similar to that of group two, but one lepton a little more momentum than the other. $m_{q_<l(high)}$ in group four will be in the little position and will be larger than $m^{\max}_{q_<l(low)}$. By varying the angle between the leptons with each other and with the quarks further configurations can be found with bigger values of $m_{ql(LITTLE)}$ than $m^{\max}_{q_<l(low)}$. However $m_{ql(LITTLE)}$ will never be as big as $\min\{m^{\max}_{q_>l(low)}, m^{\max}_{q_<l(high)}\}$ which is the third highest of the unobservable endpoints.

Tiny endpoint

$m^{\max}_{ql(tiny)} = m^{\max}_{q_{<}l(low)}$ and so will originate from events in group two. If the far quark has the lower momentum, group three will produce the same endpoint as group two, but never a higher one. No event can result in a higher $m_{ql(TINY)}$, as in order to be the smallest m_{ql} it must be due to the smaller $m_{ql(Low)}$ for that event, which cannot be bigger than $m^{\max}_{q_{<}l(low)}$ by definition. Therefore $m^{\max}_{ql(tiny)}$ is equal to the smallest unobservable endpoint.

Summary

- $m^{\max}_{ql(HUGE)} = \max\{m^{\max}_{q_{near}l(high)}, m^{\max}_{q_{far}l(high)}\} = m^{\max}_{q_{>}l(high)}$
- $m^{\max}_{ql(LARGE)} = \max\{m^{\max}_{q_{>}l(low)}, m^{\max}_{q_{<}l(high)}\}$
- $m^{\max}_{ql(TINY)} = \min\{m^{\max}_{q_{near}l(low)}, m^{\max}_{q_{far}l(low)}\} = m^{\max}_{q_{<}l(low)}$

The qql endpoints

This is approached in the same way as the ql edges with the two quarks together as an effective particle.

High endpoint

The event that maximises $m_{qql(high)}$ has one lepton at rest and the other back to back with both the quark effective particle and $\tilde{\chi}_1^0$ in the $\tilde{\chi}_2^0$ rest frame.

The mass of the effective particle is

$$m_{qq}^2 = \lambda(m_{\tilde{g}}^2 - m_{\tilde{q}}^2)(m_{\tilde{q}}^2 - m_{\tilde{\chi}_2}^2)/m_{\tilde{q}}^2 \qquad \lambda \in [0,1]$$

From [h]

$$(m_{qql(high)})^2 = m_{qq}^2 + 2L^{\tilde{\chi}_2}(E_{qq}^{\tilde{\chi}_2} + P_{qq}^{\tilde{\chi}_2})$$

which equals

$$(m_{qql(high)})^2 = m_{qq}^2 + \frac{m_{\tilde{\chi}_2}^2 - m_{\tilde{\chi}_1}^2}{2m_{\tilde{\chi}_2}^2}(m_{\tilde{g}}^2 - m_{\tilde{\chi}_2}^2 - m_{qq}^2 + \sqrt{(m_{\tilde{g}}^2 + m_{\tilde{\chi}_2}^2 - m_{qq}^2)^2 - 4m_{\tilde{g}}^2 m_{\tilde{\chi}_2}^2})$$

A16

This must be differentiated with respect to λ and set to zero to find the value of m_{qq}^2 that maximises A16.

$$m_{qq}^2 = (m_{\tilde{g}}^2 + m_{\tilde{\chi}_2}^2 - \frac{m_{\tilde{g}}}{m_{\tilde{\chi}_1}}(m_{\tilde{\chi}_2}^2 + m_{\tilde{\chi}_1}^2) \quad \text{A17}$$

Substituting this back into A16 yields,

$$(m_{qql(high)}^{\max})^2 = (m_{\tilde{g}} - m_{\tilde{\chi}_1})^2$$

The edges produced when the qq invariant mass is at its extreme values must also be found.

λ=0 gives;

$$(m_{qql(high)}^{\max})^2 = (\frac{(m_{\tilde{g}}^2 - m_{\tilde{\chi}_2}^2)(m_{\tilde{\chi}_2}^2 - m_{\tilde{\chi}_1}^2)}{m_{\tilde{\chi}_2}^2})$$

Substituting $m_{qq} = m_{qq}^{\max}$ into A16, yields

$$(m_{qql(high)})^2 = \frac{(m_{\tilde{g}}^2 - m_{\tilde{q}}^2)(m_{\tilde{q}}^2 - m_{\tilde{\chi}_2}^2)}{m_{\tilde{q}}^2} + \frac{m_{\tilde{\chi}_2}^2 - m_{\tilde{\chi}_1}^2}{2m_{\tilde{\chi}_2}^2}(m_{\tilde{q}}^2 - 2m_{\tilde{\chi}_2}^2 - \frac{m_{\tilde{g}}^2 m_{\tilde{\chi}_2}^2}{m_{\tilde{q}}^2} + \frac{1}{m_{\tilde{q}}^2}\sqrt{(m_{\tilde{q}}^4 - m_{\tilde{g}}^2 m_{\tilde{\chi}_2}^2)^2})$$

which results in two solutions, depending on the sign of $m_{\tilde{q}}^4 - m_{\tilde{g}}^2 m_{\tilde{\chi}_2}^2$

$$(m_{qql(high)}^{\max})^2 = (\frac{(m_{\tilde{g}}^2 - m_{\tilde{q}}^2)(m_{\tilde{q}}^2 - m_{\tilde{\chi}_1}^2)}{m_{\tilde{q}}^2}) \quad \text{where } m_{\tilde{q}}^2 \le m_{\tilde{g}} m_{\tilde{\chi}_2}$$

$$(m_{qql(high)}^{\max})^2 = (m_{\tilde{q}}^2 - m_{\tilde{\chi}_2}^2)(\frac{m_{\tilde{g}}^2 m_{\tilde{\chi}_2}^2 - m_{\tilde{q}}^2 m_{\tilde{\chi}_1}^2}{m_{\tilde{q}}^2 m_{\tilde{\chi}_2}^2}) \quad \text{where } m_{\tilde{q}}^2 \ge m_{\tilde{g}} m_{\tilde{\chi}_2}$$

By finding the λ<1 and λ>0 boundaries, that is when A17 $< m_{qq}^{\max}$ or A17>0, the three endpoints corresponding to the extreme λ values can be assigned mass regions.

$(m_{qql(high)}^{\max})^2 = (\frac{(m_{\tilde{g}}^2 - m_{\tilde{\chi}_2}^2)(m_{\tilde{\chi}_2}^2 - m_{\tilde{\chi}_1}^2)}{m_{\tilde{\chi}_2}^2})$	$m_{\tilde{\chi}_2}^2 \ge m_{\tilde{g}} m_{\tilde{\chi}_1}$
$(m_{qql(high)}^{\max})^2 = (\frac{(m_{\tilde{g}}^2 - m_{\tilde{q}}^2)(m_{\tilde{q}}^2 - m_{\tilde{\chi}_1}^2)}{m_{\tilde{q}}^2})$	$m_{\tilde{q}}^2 \le m_{\tilde{g}} m_{\tilde{\chi}_1}$

$(m^{\max}_{qql(high)})^2 = (m^2_{\tilde{q}} - m^2_{\tilde{\chi}_2})(\frac{m^2_{\tilde{g}} m^2_{\tilde{\chi}_2} - m^2_{\tilde{q}} m^2_{\tilde{\chi}_1}}{m^2_{\tilde{q}} m^2_{\tilde{\chi}_2}})$	$m^2_{\tilde{q}} m_{\tilde{\chi}_1} \geq m_{\tilde{g}} m^2_{\tilde{\chi}_2}$
$(m^{\max}_{qql(high)})^2 = (m_{\tilde{g}} - m_{\tilde{\chi}_1})^2$	Otherwise

Low endpoint

The low edge was approached in exactly the same way as the high edge, but with the lepton energy halved to give the low configuration, which has identical leptons back to back with the quark.

Following the algebra as above yields

$m^2_{qq} = m^2_{\tilde{g}} + m^2_{\tilde{\chi}_2} - \frac{m_{\tilde{g}}}{\sqrt{2(m^2_{\tilde{\chi}_2} + m^2_{\tilde{\chi}_1})}}(3m^2_{\tilde{\chi}_2} + m^2_{\tilde{\chi}_1})$ replacing A17.

Four endpoints which are very similar to the high expressions are derived. The only difference is that the mass of $\tilde{\chi}^0_1$ is replaced by $\sqrt{\frac{m^2_{\tilde{\chi}_2} + m^2_{\tilde{\chi}_1}}{2}}$

Further investigation showed that if $\tilde{\chi}^0_1$ is produced at rest and the leptons are back to back in the $\tilde{\chi}^0_2$ frame, $m_{qql(low)}$ can be maximised when $m^{\max}_{qq}$ is perpendicular to the leptons.

From [h]

$(m_{qql(high)})^2 = (m^{\max}_{qq})^2 + 2L^{\tilde{\chi}_2}(E^{\tilde{\chi}_2}_{qq})$ A18

As $\tilde{\chi}^0_1$ is at rest both the leptons have momentum $L^{\tilde{\chi}_2} = \frac{(m_{\tilde{\chi}_2} - m_{\tilde{\chi}_1})}{2}$ and so A18 is calculated to be

$(m^{\max}_{qql(low)})^2 = m_{\tilde{\chi}_2} m_{\tilde{\chi}_1} + m^2_{\tilde{g}} - (m_{\tilde{\chi}_1} + m_{\tilde{\chi}_2})(\frac{m^2_{\tilde{g}} m^2_{\tilde{\chi}_2} + m^4_{\tilde{q}}}{2m^2_{\tilde{q}} m_{\tilde{\chi}_2}})$

For this to be bigger than the four previous endpoints, the lepton energy must be big enough to compensate for the fact that it is no longer back to back with the quark effective particle.

The simulation shows that these five endpoints are not the final expressions, as they still occasionally underestimate the endpoint.

Summary

$m_{qll(low)}$	$(m^{\max}_{qql(low)})^2 = \max\{A, B\}$ $(m^{\max}_{qql(low)})^2 = \max\{A, C\}$ $(m^{\max}_{qql(low)})^2 = \max\{A, D\}$ $(m^{\max}_{qql(low)})^2 = \max\{A, E\}$ $A = m_{\tilde{\chi}_2} m_{\tilde{\chi}_1} + m^2_{\tilde{g}} - (m_{\tilde{\chi}_1} + m_{\tilde{\chi}_2})(\frac{m^2_{\tilde{g}} m^2_{\tilde{\chi}_2} + m^4_{\tilde{q}}}{2m^2_{\tilde{q}} m_{\tilde{\chi}_2}})$ $B = (\frac{(m^2_{\tilde{g}} - m^2_{\tilde{\chi}_2})(m^2_{\tilde{\chi}_2} - x^2)}{m^2_{\tilde{\chi}_2}})$ $C = (\frac{(m^2_{\tilde{g}} - m^2_{\tilde{q}})(m^2_{\tilde{q}} - x^2)}{m^2_{\tilde{q}}})$ $D = (m^2_{\tilde{q}} - m^2_{\tilde{\chi}_2})(\frac{m^2_{\tilde{g}} m^2_{\tilde{\chi}_2} - m^2_{\tilde{q}} x^2}{m^2_{\tilde{q}} m^2_{\tilde{\chi}_2}})$ $E = (m_{\tilde{g}} - x)^2$	$m^2_{\tilde{\chi}_2} \geq m_{\tilde{g}} x$ $m^2_{\tilde{q}} \leq m_{\tilde{g}} x$ $m^2_{\tilde{q}} x \geq m_{\tilde{g}} m^2_{\tilde{\chi}_2}$ Otherwise $x = \sqrt{\frac{m^2_{\tilde{\chi}_2} + m^2_{\tilde{\chi}_1}}{2}}$

Appendix B
A copy of the montecarlo event generator is included on a CD.

References

1. C Lester, Model independent sparticle mass measurements at ATLAS.
2. M White, C Lester, M Parker, Observation of three body endpoint in simulated NUHM data.
3. B. Gjelsten D. Miller, P. Osland; Measurement of the Gluino Mass via Cascade Decays for SPS 1a.
4. S. P. Martin, A Supersymmetry Primer, hep-ph/9709356